ELSEVIER

Earth and Planetary Science Letters 139 (1996) 395–409

EPSL

A scaling growth model for bubbles in basaltic lava flows

H. Gaonac'h [a,*], S. Lovejoy [b], J. Stix [a], D. Scherzter [c]

[a] *Département de Géologie, Université de Montréal, Montréal, Que., H3C 3J7, Canada*
[b] *Department of Physics, McGill University, Montreal, Que., H3A 2T8, Canada*
[c] *Laboratoire de Météorologie Dynamique, Université Pierre et Marie Curie, 4 place Jussieu, Paris Cedex 05, France*

Received 5 January 1995; accepted 20 February 1996

Abstract

Pahoehoe, aa and massive lavas from Mount Etna show common statistical properties from one sample to another which are independent of scale/size over certain ranges. The gas vesicle distribution shows two scale-invariant regimes with number density $n(V) \propto V^{-B-1}$, where V is the volume and empirically $B \approx 0$ for small bubbles and $B \approx 1$ for medium to large bubbles. We introduce a bubble growth model which explains the $B > 1$ range by a strongly non-linear cascading growth regime dominated by a quasi-steady-state coalescence process. The small bubble region is dominated by diffusion; its role is to supply small bubbles to the coalescence regime. The presence of measured dissolved gas in the matrix glass is consistent with the notion that bubbles generally grow in quasi-steady-state conditions. The basic model assumptions are quite robust with respect to the action of a wide variety of processes, since we only require that the dynamics are scaled over the relevant range of scales, and that during the coalescence process, bubble volumes are (approximately) conserved. The model also predicts a decaying coalescence regime (with $B > 1$) associated with a depletion of the gas source or, alternatively, a loss of large vesicles through the surface of the flow. Our model thus explains the empirical evidence pointing to the coexistence of two different growth mechanisms in subsurface lava flows, but acting over distinct ranges of scale, with non-linear coalescence as the primary growth process. The total vesicularity of each sample can then be well estimated from the partial vesicularity of each growth regime without any outlier problems.

Keywords: basalts; lava flows; gases; vesicular texture; growth rates

1. Introduction

1.1. Previous work

The bubble content, shape and size distributions, as well as their spatial and temporal variations, strongly affect the rheology of erupted lavas. The presence or absence of vesicles may dramatically change the viscosity and yield strength of a lava from one point to another according to the shape and size of the vesicles. When submitted to stress, such a compressible lava flow containing bubbles will flow less rapidly than an incompressible massive one [1]. This may lead to complex differential strain rates and, eventually, to fragmentation (or break-up) of the lava into fractal patterns like the 'cauliflowers' observed in aa lava at Mount Etna [2]. Furthermore, since vesicularity is highly inhomogeneous, the rheology is affected over a wide range of scales and this

* Corresponding author. E-mail: gaonach@ere.montreal.ca

PII S0012-821X(96)00039-8

must be taken into account in explaining a wide variety of heterogeneous and complex geophysical structures which have been found over a large range of scales [3–8]. Lobes, channels and levées are examples of such strong morphological variability.

In spite of their rheological significance, bubbles from basaltic lava flows have only been studied extensively in the last 10 years [9–22] and often their characterization has been reduced to mean bubble volumes. However, such averages (as used by, e.g. [14,16]) give only very partial information concerning the variation of the vesicularity (fraction of gas vesicles in the lava), the relationship between small and large bubbles in lava flow fields, or the growth processes. This is especially true since, as shown in Gaonac'h et al. [6], and below, the mean bubble volume of an individual sample is generally strongly influenced by the single largest vesicle present and, hence, will exhibit large sample-to-sample variability, masking the true volcanological variability.

Various growth mechanisms explaining the observed distributions have been suggested. For example, coalescence has been proposed [10] as a major dynamic growth process, operating by the collection of bubbles of neighbouring sizes. In contrast, Walker [14] suggested an essentially static coalescence mechanism (i.e. with bubble boundaries but not centres evolving) operating in spongy pahoehoe from Hawaii, which would be triggered by the appearance of diktytaxitic voids. Another primary mechanism was proposed by McMillan [11], Aubele et al. [12] and Carbone [13], who argued that a model based on continuous bubble growth by diffusion was adequate for explaining the vesicle sizes found in lava flows. In support of this model, Sarda and Graham [17], Mangan et al. [18], and Cashman et al. [19] analyzed the full bubble size distribution of non-degassed mid-ocean ridge basalts and Hawaiian lavas using thin sections. Based on experimental and theoretical results of crystal growth, they proposed that exponential vesicle size distributions could arise from continuous diffusion and expansion growth mechanisms. Because only a few large 'outlier' vesicles were unexplained by their exponential trends (although they contribute a large fraction of the vesicularity) they concluded that coalescence is not important compared to diffusion and expansion.

The basic problem of the pure diffusion approach in subsurface lava flows is that, for larger and larger bubbles, diffusion becomes rapidly inefficient, whereas coalescence becomes increasingly more efficient; hence the dynamic coalescence mechanism is quite seductive, at least for large enough bubbles. However, until now, the quantitative treatment of coalescence has been hampered because of its highly non-linear nature. In the present paper, we show how this difficulty can be somewhat overcome; not by appealing to a hypothetical weak non-linearity but, rather, by looking at the scaling symmetries of the dynamic processes. For the purposes of this paper, structures scale if their characteristic parameters are described by a power law with a constant exponent as a function of the scale. For example, areas and perimeters of flows were found to be scale-invariant over a range of scale from 10 m to 50 km [5]. A more precise definition is that their statistical properties at two different scales are related by the scale ratio raised to various powers [4].

1.2. Our study

Our work on basaltic lava flows [3,6] has concerned near-surface conditions where (compared to magmatic chamber conditions) decompression is not important. We have studied lavas which were systematically sampled from the source to the front of flows from the 1985 and 1991–93 eruptions of Mount Etna (Italy). The large size of our samples allows us to analyze a wide range of bubble scales observed in the field. Bubbles with volume ratios (large/small) of 10^7 are commonly observed in lava samples, including the all important large bubbles which contribute most of the vesicularity but which are treated as statistical 'outliers' in the usual approaches. The largest bubbles studied were 2400 mm^3, which are too large to be studied in thin sections. Without modifying the bubble boundaries (or in any way attempting to 'decoalesce' bubbles, see [19]), we have demonstrated that two power law functions accurately describe the entire number–size distribution of bubble populations from Mount Etna lava flows [3,6]. The two regimes intersect in a transition zone defined by a characteristic volume V^*. One important point of our study was that the analyses covered the inner and outer scales of the critical large bubble scaling regime, which is characterized

by a number density with an exponent $B \approx 1$ (the other power law is defined with $B \approx 0$):

$$n(V) \propto V^{-B-1} \quad (1.1)$$

When considering the vesicularity and number distribution (the integral of the number density), different power law regimes can be defined, depending on B values. For $B < 1$, the vesicularity is dominated by contributions from the large bubbles. For $B < 0$, the number distribution itself is dominated by the large bubbles. The regime $0 \leq B \leq 1$ (of interest here) thus has the apparently contradictory properties of having numerous small bubbles that dominate the number distribution, while simultaneously having large bubbles which contribute a dominant proportion of the total vesicularity. The special case $B = 1$ involves both a significant contribution of small and large vesicles to the vesicularity. In this case, we also obtain a scale-invariant property of the spatial vesicle patterns; that is, they have fractal structures over the corresponding range of scales. Hence, for $B \leq 1$, the variability in the vesicularity is significantly affected by the presence or absence of a few, rare, large vesicles (bubbles) in the sample (even with $B > 1$ the variability can be large).

In contrast, a Hawaiian spongy pahoehoe demonstrated a unique power law, with an exponent $B \approx +0.2$ for all bubble sizes [3,6]. This is not surprising since Walker [14] has suggested a different cooling history for the Hawaiian lava than for samples from Mount Etna; the growth mechanism of Hawaiian lavas probably did not include many bubble collisions.

We suggest here that the power law function (empirically with exponent $B \approx 0$) acting in the small-bubble range of sizes may be explained by diffusion growth, while the power law function with the exponent $B \approx 1$, existing for the medium to large vesicles, may be associated with a coalescence regime. Using scaling symmetries, we define the different regimes where diffusion or coalescence dominate and estimate their respective contributions to the overall vesicularity. In quasi-steady-state conditions, the coalescence may be explained by a cascading series of collisions, each involving an approximate volume conservation. This model yields $B \approx 1$ and may apply not only to a cascading series of coalescence of bubbles, but possibly also to the breakup bubbles (an inverse cascade), or both simultaneously. When the quasi-steady-state conditions do not prevail any longer, the scaling model predicts the existence of a new bubble growth regime with $B > 1$. The quasi-steady-state may be highly intermittent; it need only be statistically steady, with large fluctuations occurring at any moment.

2. A scaling cascade model

2.1. The coalescence equation

Bubble dynamics are highly non-linear, depending on the multiple interaction of bubbles (either directly or via the flow field). The simplest models reduce the problem to binary interactions [1] in an otherwise stationary flow field, and exploit the coalescence (Smoluchowski) equation to model the number density $n(V,t)$ (e.g., [10]). Due to the non-linear nature of these models, they are prone to numerical instabilities and will be highly dependent on boundary conditions, such as the initial distribution of bubbles, which are never known with precision. Furthermore, the exact solutions of the equations will depend strongly on the existence and type of bubble heterogeneity. One may also criticize the appropriateness of the coalescence because: (1) direct observations of bubble growth in dynamically evolving lava flows or magma chambers are not available; and (2) alternative mechanisms such as that postulated for bubble distributions in the ocean may be more relevant (i.e. break-up or 'inverse coalescence'). However, since the non-linear growth equations generally obey scaling symmetries (as may the flow itself), the solutions may be expected, at least statistically, to respect the same symmetries; hence, many of these problems can be partially overcome. It is, therefore, important to stress at the outset that our model depends essentially only on a cascade of interactions respecting scaling and volume conservation; it is more general than the coalescence equation. The latter is employed primarily as a

[1] Manga and Stone [22], underline that the characterization of two-particle interaction provides a useful model for understanding the behaviour of systems with many bubbles.

convenient concrete framework for illustrating our ideas.

Ignoring bubble sources and sinks other than those provided by the coalescence process itself, the coalescence equation may be written as:

$$\frac{\partial n(V,t)}{\partial t} = \frac{1}{2}\int_0^V H(V-V',V')\,n(V-V',t)\,n(V',t)\,\mathrm{d}V' - n(V,t)\int_0^\infty H(V,V')\,n(V',t)\,\mathrm{d}V' \qquad (2.1)$$

where H, the 'coagulation coefficient', is the probability of two bubbles with size V and V' coalescing per unit time. This coagulation coefficient is given by:

$$H(V,V') = E(V,V')\left(V^{\frac{1}{3}} + V'^{\frac{1}{3}}\right)^2 |u(V) - u(V')| \qquad (2.2)$$

where u is the bubble velocity, and E is the collision efficiency, which determines the fraction of collisions resulting in coalescence. The middle term is purely geometric and takes into account the bubble cross-sections. Although this term is usually derived for spherical particles or bubbles, the assumption of statistical isotropy which is effective for Mount Etna bubbles (see [3]) is here probably sufficient, but then H must be considered as an average or 'effective' coefficient. The first term on the right-hand side of Eq. (2.1) is the rate of production of bubbles of size V via collisions of two bubbles of volumes $(V-V')$ and V' (the factor $1/2$ is to avoid double counting). The second term is the rate of loss of bubbles of size V due to collisions of bubbles of size V. If sources or sinks of bubbles arising from processes other than coalescence are considered for bubble growth, we may add other terms to the right side of Eq. (2.1).

With some rather mild assumptions about the collision efficiency E and velocity u, we can readily determine the scaling symmetries and estimate the scaling exponents. In a different context, this has recently been done by Meunier and Peschanski [23], who have shown how this equation can lead to multifractal statistics in high energy particles. This connection with multifractals is an important step forward in understanding coalescence processes and underlines the fact that enormous fluctuations are expected in coalescence processes. This is certainly compatible with the results found in lava flows, where both the distribution of bubbles and the overall porosity vary considerably from place to place, even for samples located very near to each other [3].

2.2. Scaling properties of the coalescence equation

In fluid problems, the velocity is usually assumed to be a power law of the radius or volume; from dimensional analysis it can often be shown that:

$$u(V) \propto V^{\gamma} \qquad (2.3)$$

For example, for Newtonian fluids in the high Reynolds number (Re) limit (large velocity, low viscosity), the drag coefficient becomes constant, implying that $\gamma = \frac{1}{6}$ [24]. At low Re, the drag coefficient becomes inversely proportional to the Reynolds number leading to $\gamma = \frac{2}{3}$. The latter case is more relevant to bubbles in lava since [2] $Re \ll 1$, although both results are only strictly valid for single bubbles acting under the influence of gravity in an otherwise static fluid.

For a Bingham fluid, it is possible that the γ value is not affected. In the more general case new dimensional quantities will be introduced and γ will, presumably, be affected. We show below that the exact value of γ is not important as long as it is larger than $1/3$. In any case, if the bubbles are in a complex flow field, statistical exponents may be required.

[2] When regarding the viscosity, the critical value $Re = 1$ leads to the dissipation length scale of $d_{\mathrm{dis}} = \frac{\eta}{u\rho}$ where η is the lava viscosity, ρ its density and u the average velocity of the bubble moving in the flow; the ratio will actually be highly variable, since, for a fixed bubble size, u and η will not be constant, due to the complex velocity and temperature fields respectively. Although clearly use of 'typical values' to estimate d_{dis} is a great simplification, it here demonstrates that the viscous length need not worry us. Using typical values $\eta \approx 10^2 - 10^4$ Pas [9], $u \approx 10^{-3} - 10^{-1}$ ms^{-1} (these are the velocities of the bubble with respect to the mean flow), $\rho \approx 3 \times 10^3$ k gm^3, we obtain $d_{\mathrm{dis}} \approx 30$ cm–3 km, i.e. much larger that our range of interest. This result is in agreement with $Re \ll 1$, where the relevant dynamics are dominated by the viscosity. A priori, as far as the direct effects of viscosity is concerned, they will be scaling.

In many applications (e.g. drop collision in meteorology), it is usually assumed that the mechanism determining collision efficiency is only a function of the ratio of the sizes [10]:

$$E(V,V') = E\left(\frac{V}{V'}\right) \tag{2.4}$$

Under these conditions, the dynamics are scaling because no characteristic volume appears in Eq. (2.1) [3]. Under appropriate boundary conditions (i.e. which do not impose a characteristic size/volume in the size range of interest), the equation will allow scaling solutions for the number density of the form (where we use the subscript c to indicate 'coalescence'):

$$n(V,t) \propto V^{-B_c-1} t^{-\xi} \tag{2.5}$$

To determine the values of the exponents B_c and ξ, we substitute Eq. (2.5) into Eq. (2.1). The differentiation of the left-hand side of Eq. (2.1) leads to:

$$\frac{\partial n(V,t)}{\partial t} \propto V^{-B_c-1} t^{-\xi-1} \tag{2.6}$$

Note that it is the integral of $n(V)$ (the number distribution) which is most conveniently empirically estimated (see [6]). Next, we evaluate the corresponding right-hand side of Eq. (2.1) by simply changing the variables in the above integrals, obtaining (see details in Appendix A:

$$\frac{\partial n(V,t)}{\partial t} \propto V^{\gamma-\frac{1}{3}-2B_c} t^{-2\xi} \tag{2.7}$$

Comparing Eq. (2.6) and Eq. (2.7), we obtain:

$$B_c = \frac{2}{3} + \gamma$$
$$\xi = 1 \tag{2.8}$$

[3] In this model the complex non-linear effects associated notably with viscosity and surface tension will be implicitly accounted for by their effect on E. All we require is that these effects lead to a scaling function: $E(\lambda V,\lambda V') = \lambda^s E(V,V')$ where s is a new scaling exponent and λ is the zooming/magnification ratio. As illustrated in Eq. (2), E is commonly taken to be a function of the ratio of the sizes; thus $s=0$, a simplification which (in the absence of more information) we adopt here.

Solutions with this time dependence (i.e., $n(V,t) \propto t^{-1}$) will be relevant when no new sources of bubbles are present, and the overall number decreases ($\frac{\partial n(V,t)}{\partial t} < 0$) only via the coalescence mechanism. Such solutions are likely to be relevant when diffusive degassing of the lava is nearly finished. Using $\gamma = \frac{2}{3}$ for lavas will lead to $B_c > 1$ for such pure coalescence.

2.3. Competition between diffusion and coalescence

We now consider scaling solutions in quasi-steady-state situations ($\frac{\partial n(V,t)}{\partial t} \approx 0$), where the overall number does not change. This may be the case when diffusive growth of small bubbles provides a near-constant source of gas to the coalescence regime. Under these conditions, we can still have scaling solutions, but with $\xi = 0$; B_c will no longer be determined by the balance of the two right-hand side terms of Eq. (2.1). In this situation, we argue that B_c will be determined by the quasi-steady flux originating at diffusive scales and the non-linear bubble coalescence interactions which conserve the volume of gas.

In order for there to exist a quasi-steady-state coalescence regime ($\frac{\partial n(V,t)}{\partial t} \approx 0$), we must first establish that a diffusive regime capable of providing the small bubble source can, in fact, exist. Due to complex nucleation processes, some initial distribution of small bubbles arises. We may then use the standard analysis of diffusive growth [16], which relates the rate of increase in volume to the volume itself:

$$\frac{dV}{dt} \propto V^{\epsilon} \tag{2.9}$$

The standard 'parabolic' growth law corresponds to growth of isolated bubbles and yields $\epsilon = 1/3$. This law is valid for a single bubble or for the approximate case where neighbouring bubbles are not interacting [16]. Alternatively, if diffusion involves the non-linear interaction of neighbouring bubbles (Ostwald ripening) we obtain $\epsilon = 0$.

Using dimensional analysis, this equation gives the following diffusive time scale:

$$\tau_d \approx V\left(\frac{dV}{dt}\right)^{-1} \approx V^{1-\epsilon} \tag{2.10}$$

Once again, we have ignored dimensional proportionality constants, concentrating instead on the scaling exponents.

Similarly, the coalescence time scale may be estimated as:

$$\tau_c \approx n(V,t)\left(\frac{\partial n(V,t)}{\partial t}\right)^{-1} \approx V^{B_c-\frac{2}{3}-\gamma} \qquad (2.11)$$

where, since we are only interested in the scaling, we have estimated τ_c by using the second term of Eq. (2.1). The two right-hand terms of Eq. (2.1) are of identical order, since their sum gives the steady-state condition $\frac{\partial n(V,t)}{\partial t} \approx 0$.

Comparison of Eq. (2.10) and Eq. (2.11) shows that, for $B_c < \gamma + \frac{5}{3} - \epsilon$, the diffusive time scale for small enough bubbles will be much shorter than the coalescence time scale and will dominate. By contrast, for larger and larger bubbles, diffusion quickly becomes inefficient. Furthermore, if $B_c < \frac{2}{3} + \gamma$ (e.g., $\gamma \approx 2/3$ and $B_c \approx 1$), then τ_c decreases with increasing V, and coalescence becomes more rapid for larger bubbles. These conditions may well be appropriate for medium to large bubbles in our samples from Mount Etna [3]. If a quasi-steady-state regime with $B_c < \frac{2}{3} + \gamma$ and $\xi = 0$ is interrupted (e.g. the source of bubbles becomes exhausted) and only pure coalescence operates (called a decaying regime), then a regime with $B_c = \frac{2}{3} + \gamma$ and $\xi = 1$ will establish itself first at large V, since the large bubble part of the coalescence regime evolves the fastest (τ_c is smallest).

2.4. The role of surface tension

Before proceeding, we also have to consider the possible role of another characteristic time which may be important; the coagulation time scale, $\tau_{coag} \approx V^{1/3}$ [20]. This is the time scale for the liquid film between colliding bubbles to be ruptured, and depends on the viscosity of the lava and surface tension of the bubble. Because the coagulation exponent $1/3 > B_c - 2/3 - \gamma$ (see Eq. (2.11)), for large enough bubbles, the coagulation process will be slower than the collision process, and could potentially disrupt it.

However, this complication is not necessarily too significant for our model. All that the latter requires is that bubbles which have experienced a collision (and are thus in close contact) have effectively coalesced. All that the model requires is that, as far as future coalescence events are concerned, they may henceforth be considered as a single bubble — even if the viscous film between them has not completely retracted. Such partially coalesced bubbles are indeed observed in natural samples. Bubbles with such internal films will be able to participate further on in the cascade growth coalescence without greatly changing the model assumptions. Hence, the coagulation process does not necessarily qualitatively affect the model presented here or change the exponent determined from conservation laws as described below.

We have already argued that, because scaling is a dynamic symmetry principle, it will be respected in the absence of a specific scale breaking mechanism. In principle, both viscosity and surface tension can introduce characteristic lengths to specifically characteristic bubble sizes when respectively the Reynolds (*Re*, see [9]) and Capillary numbers (*Ca*, see [19,20]) approach unity. We have already seen that the viscous dissipation scale (where $Re \approx 1$) is much larger than our scales of interest, it need not concern us further. Turning our attention to the surface tension, it will act to inhibit the deformation of bubbles. Bubbles whose capillary number $(Ca) \geq 1$ are deformable whereas those with $Ca \leq 1$ are relatively non-deformable and thus more spherical. A basic problem is that meaningful estimates of *Ca* in real lava flows are difficult if not impossible; it is usually assumed that deformation does not play a significant role (by implication, $Ca < 1$). Indeed, in real lava, *Ca* is likely to vary widely as a function of location. For example, in a laboratory setting, Manga and Stone [22] have estimated that deformation only occurs for bubbles with a radius larger than 5 mm, and that deformation of isolated bubbles will increase the rate of coalescence. In contrast, Gaonac'h et al. [6] observed that, except for very small vesicles, bubbles typically have complex forms, either due to deformation or coagulation effects; indeed, the two effects are not obviously separable in solid lava samples [4]. The effect of possible deformability

[4] Indeed, we have already noted that, when $B = 1$, the spatial vesicle patterns will be fractal, a result which, in principle, could have involved only purely spherical bubble collisions.

is not clear. In any case, this issue has little direct impact on the quasi-steady-state model, since the collision time scale is set by the small bubble source and any growth mechanism which preferentially tends to increase the rate of large bubble collisions will not affect the cascade process described below.

2.5. The quasi-steady-state regime and the cascade model

In a quasi-steady-state ($\frac{\partial n(V,t)}{\partial t} \approx 0$), B_c is not determined by the coalescence equation itself; it will depend on boundary conditions, especially the sources of the small bubbles. In order to analyse this situation, we first note that the coalescence equation has a quadratic non-linearity, which is analogous in many ways to the non-linearity in the fluid (Navier–Stokes) equations. In particular, the bubble analogue of a 'direct' turbulent cascade of energy flux from large to small scales is the 'inverse' cascade involving the growth of large bubbles by coalescence. Such a cascade will occur when the most efficient growth mechanism of a large bubble is via a succession of collisions of not too dissimilar sized bubbles, rather than via a single medium-sized drop sweeping up large numbers of much smaller drops. A precise formulation of this dichotomy is the notion of local/non-local bubble interactions. This jargon indicates whether or not the strongly interacting structures have neighbouring wavenumbers in Fourier space; it refers to Fourier space locality, not physical space locality. In the case where the interaction is local (as we will argue here), then the dynamics need only be studied over a limited range of scales (denoted λ_0), since, due to the scaling, the same mechanism then repeats iteratively to produce larger and larger bubbles. Although over this range, only 'direct' interactions within a size range λ_0 are explicitly taken into account (Fig. 1a), due to the iteration, indirect interactions (over ranges λ_0^2, λ_0^3, etc.) are implicitly accounted for (Fig. 1b). Empirically, many authors (notably Sahagian [10] and Manga and Stone [22]) have noted the extreme inefficiency of bubble coalescence for collisions involving bubbles of very different sizes. The small bubble is simply entrained around the larger one without coalescence occurring. This makes it likely that the interactions are indeed local. In the next section we quantify this.

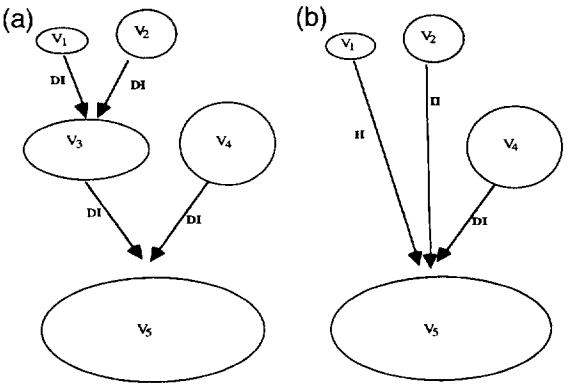

Fig. 1. (a) Scheme of direct interactions (DI) between pairs of bubbles. (b) Scheme of direct (DI) and indirect interactions (II) between three bubbles leading to the same final size of bubble as in (a).

2.6. The locality / non-locality of bubble interactions

In considering the issue of locality/non-locality in the quasi-steady cascade model (dropping the time dependence), it is sufficient to consider the production term of Eq. (2.1):

$$Q = \frac{1}{2}\int_0^V H(V-V',V')\,n(V-V')\,n(V')\,\mathrm{d}V' \tag{2.12}$$

Since we are considering the scaling functions indicated in the previous sections, we will consider the case $V = 1$ (the scaling relations detailed in Appendix A can then be used to determine the production for any other V). The volume ratio of the two coalescing drops is expressed as $\lambda = V'/(1-V')$. Since the two drops are physically equivalent, the above must be symmetric under exchange of the volumes (i.e. $V' \to 1-V'$, $1-V' \to V'$ and hence symmetric under $\lambda \to 1/\lambda$). We consider the special case Eq. (2.4) and note that by this symmetry $E(\lambda) = E(\lambda^{-1})$. Hence, we need only consider the range $\lambda \geq 1$. We therefore obtain:

$$Q = \int_1^\infty E(\lambda)|1-\lambda^{-\gamma}|(1+\lambda^{-1/3})^2 \times (1+\lambda^{-1})^{2B-\gamma-2/3}\lambda^{-1+B}\,\mathrm{d}\lambda \tag{2.13}$$

The question of 'locality' of the interactions can now be addressed precisely. The cascade can be considered 'local' if a finite scale ratio λ_0 exists

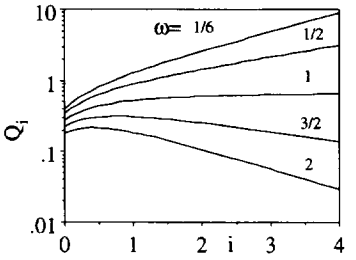

Fig. 2. Diagram of the production term, log Q_i, due to contributions of all the bubbles with size ratios within an octave. The ordinate is $\log_2 \lambda$, where λ is the bubble size ratio; Q_i is the production (see Eq. (2)) numerically integrated over the range $\lambda = 2^i$ to $\lambda = 2^{i+1}$. The value of $B = 1$ was used; according to the analysis in the text, the critical value of ω therefore equals 1. For $\omega \leq 1$, Q_i diverges with i and the cascade is non-local; for $\omega > 1$, it is local. Even using the modest value $\omega = 3/2$, we see that most of the production occurs due to interactions in the first band. Note also that the straight line asymptotes are expected; on this log–log plot, they have slopes $\omega - B$.

such that most of the production of bubbles (i.e. most of the contribution to the above integral) occurs for ratios $\lambda < \lambda_0$. This will be the case for some λ_0 as long as the integrand above falls off quickly enough as $\lambda \to \infty$. If the large λ behaviour of the collision efficiency is bounded above by $E(\lambda) \approx \lambda^{-\omega}$ then ω characterizes the collision efficiency for greatly differing bubble volumes. As ω gets larger, the efficiency becomes lower and lower; larger and larger ω is, therefore, associated with more and more local interactions. We now find by inspection of Eq. (2.13) (recalling $\gamma > 0$) that the cascade will be local (i.e. the contribution to Q for large enough λ will be arbitrarily small) as long as:

$$\omega > B \tag{2.14}$$

Empirically, we found $B \approx 1$ [6]. In comparison, the only relevant data on efficiencies of which we are aware [22] concern deformable bubbles. On semi-empirical grounds (involving only a dozen or so data points), [22] suggest a formula involving two exponents, $B = 1/6$, $B = 2$ (i.e. corresponding to non-local and local behaviour respectively. Fig. 2 shows, for various values of ω, the contribution to the total production, Q, due to collisions within a single octave of volume ratios, showing that even for a relatively slow fall-off in efficiency (e.g., $\omega = 3/2$), that most of the contribution occurs within the first octave. The only other available information comes from the theoretical analysis of two isolated bubbles under the influence of gravity in an otherwise static fluid. For example, Zhang and Davis [25] (who give extensive numerics), comment on the rapid fall-off of E for large λ (due to the entrainment of small bubbles), providing general formulae of an exponential form — implying $\omega = \infty$ (their λ is our $\lambda^{-1/3}$). However, the validity of their results for $\lambda \gg 1$ is not clear. For the moment, we must therefore consider that the locality/non-locality of the cascade is an unsolved problem, although the locality hypothesis seems to be quite consistent with the available theoretical and empirical data. Future experiments should be able to estimate ω and settle this issue.

2.7. Conservation and exponents in bubble cascades

If the cascade is local, we have argued that it is sufficient to consider a finite band with scale ratio λ_0. To make these ideas concrete, consider dividing the coalescence regime into bands increasing by factor of $\lambda_0 = 2$ in volume where bubbles may coalesce (the following argument is analogous to standard arguments used in studying turbulent cascades [26]). Under these circumstances, growth primarily occurs via a series of successive binary collisions or 'triangular' interactions between the two colliding bubbles and the newly coalesced bubble. Scale by scale iteration of this mechanism yields a 'cascading' hierarchy in which not very different sized bubbles collide to form larger ones, the new bubbles repeating the process to larger and larger sizes (Fig. 1). Other mechanisms (such as diffusion) will tend to make the interactions more non-local, but will not necessarily alter this picture. The final ingredient which is necessary to obtain the resulting scaling exponent is a conservation principle; in turbulence it is the energy flux to smaller scales which is conserved. In the bubble model, the corresponding principle is that of conservation of gas volume during each collision. Just as in turbulence, we must distinguish two different types of conservation. The first, 'microcanonical' conservation, involves strict conservation at each step of the cascade, on each individual realization of the process. This is not strictly realistic; just as in turbulence where there is a certain forcing/dissipation of structure at different scales,

here, bubbles/structures are exchanging gas fluxes with a kind of reservoir at all scales; not only directly with other structures/bubbles. A priori, just as in turbulence, it is therefore more appropriate to consider the less restrictive 'canonical conservation', which applies only on average over a statistical ensemble of identical cascading systems. The difference between the two types of conservation is that fluctuations about the mean behaviour are much larger in the case of canonical conservation.

Starting at the smallest volume V^* (Fig. 3), the ith band with bubbles of volume $V_i \approx 2^i V^*$ is defined by:

$$2^{i-\frac{1}{2}} V^* \leq V < 2^{i+\frac{1}{2}} V^* \quad (2.15)$$

$$N_i = N\left(2^{i-\frac{1}{2}} V^* \leq V < 2^{i+\frac{1}{2}} V^*\right) \propto V_i^{-B_c} \quad (2.16)$$

Bubbles with a typical band volume $V_i \approx 2^i V^*$ will be the result of n successive collisions; the rate of the overall 'cascading' process will, therefore, be determined by the band with the lowest collision rates. Since for $B_c < \frac{2}{3} + \gamma$, τ_c decreases with increasing size, the limiting rate will be that of the smallest band, which is also equal to the diffusion rate for the largest bubbles in the diffusion regime. In these scaling cascade regimes, assuming statistical isotropy, we do not expect the bubble shapes to affect our exponents; this is a consequence of our assumption of scale invariance (it will, of course, affect the rates but, if the regime is scale invariant, each band will be affected in the same way). If anisotropic scale invariance holds, as it might do if the system has differential stratification or rotation, the model can readily be appropriately generalized.

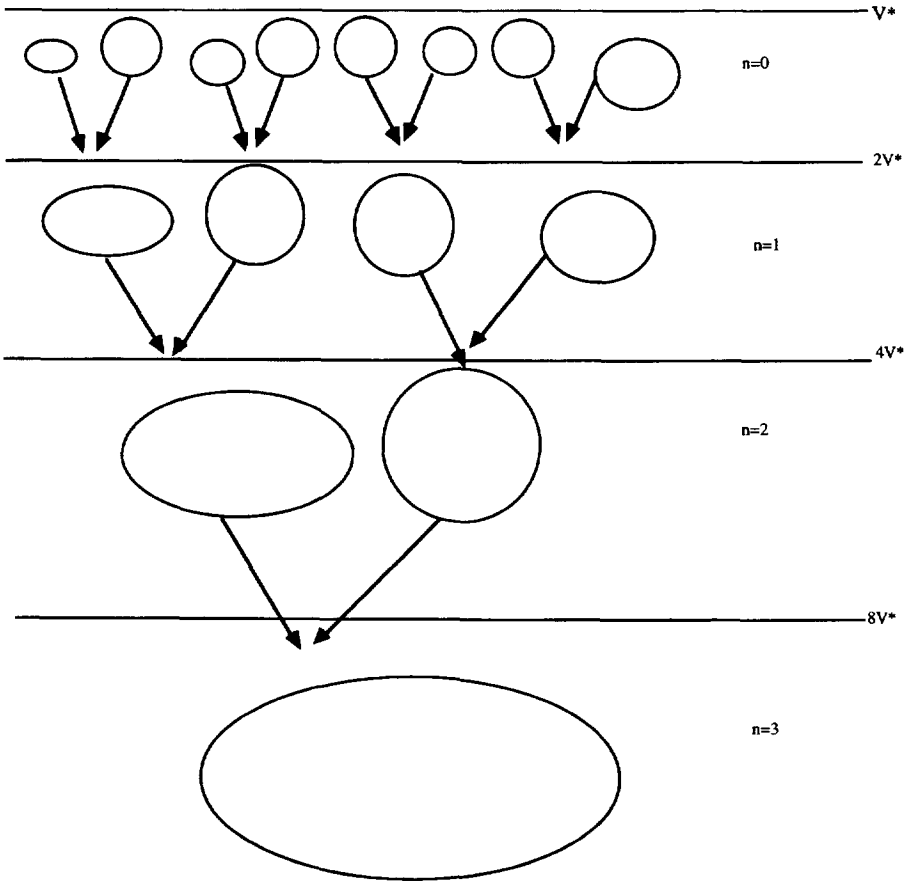

Fig. 3. Schematic view of a colliding cascade, starting with 2^3 bubbles of volume V^*, of variable shape, and ending with one bubble of volume $2^3 V^*$.

During one collision time, we therefore see that the total number of bubbles is halved while their volumes are on average doubled. Hence, this overall scale by scale volume conservation leads to the basic cascade relation:

$$N_{n+1}V_{n+1} = V_nN_n \tag{2.17}$$

From (2.16) and (2.17), we thus obtain $B_c = 1$ as a basic equation for cascading bubble growth.

For large bubbles, the equation could be equally applicable to a local cascade in which large bubbles break up into progressively smaller bubbles. Furthermore, there is no reason why break-up and its reverse (coalescence) could not co-exist to varying degrees in both systems, as it does in 3-D hydrodynamic cascades, where the direction of energy flux is only on average from large to small (the 'direct cascade'). Due to backscatter mechanisms, energy flux can fluctuate, occasionally going in the opposite direction from small to large (the 'inverse cascade'). Several relevant mechanisms have been suggested. For example, Wilmoth and Walker [15] suggested growth of bubbles in lavas by shearing, leading eventually to strong deformation and bubble loss at the surface; Stein and Spera [27] mentioned two different types of bubble break-up when stress is applied to an emulsion. Since the present (inverse, coalescence) bubble cascade will obey the same conservation laws as the direct (break-up) cascade, the resulting distributions may be the same; certainly, the two possibilities will be very difficult to distinguish empirically. In this way — although apparently sharing few features with lava bubbles — ocean bubble dynamics may provide an example of such an inverse cascade [28,29]; $B \approx 1$ is also found. As long as the growth of large bubbles depends on a cascade of collisions/break-up between bubbles with not too dissimilar sizes, the resulting $VN(V) =$ constant is likely to hold, even if collisions are not completely restricted to the same size band.

We now generalize the model somewhat to allow for exponents different than unity (c.f. the more accurate empirical estimate $B_c \approx 0.85$ [6]). This could reflect the action of other (non-local) scaling processes such as diffusion (including Ostwald ripening), which will simultaneously occur between bubble collisions. Assuming that the overall net effect of non-coalescence (and non-local) processes is to increase the bubble sizes by the factor $1+f$ during each collision, as long as $|f|$ is not too big, coalescence (i.e. local interactions) may still be considered as the dominant growth process. Repeating the above arguments but with $V_{n+1} = 2(1+f)V_n$ (instead of $V_{n+1} = 2V_n$), we obtain $B_c = \frac{\log 2}{\log 2 + \log(1+f)} \approx 1 - \frac{f}{\log 2}$ for $f \ll 1$. We see that the result $B_c \approx 0.85$ corresponds to a fractional intercollision growth (f) of $\approx 10\%$. This may explain the small variation we encounter in estimating the B_c values [6]. Furthermore, unlike the coalescence equation, which considers only pairs of bubbles, there is no reason to expect this cascade result to change due to the existence of higher order bubble–bubble interactions, which may affect the flow field in a non-linear fashion.

2.8. *Diffusion as a source of coalescence*

To make the picture entirely plausible, we need only to show that the diffusive regime can indeed supply sufficient gas to the small bubbles to maintain the overall process in a quasi-steady-state. In order for the cascading idea to be valid, the large bubble end of the diffusion regime V^*, which in this picture coincides with the small bubble end of the coalescence regime, should have the greatest diffusive flux into it; if not, the steady-state conditions would be stopped or 'choked' due to lack of gas from the diffusive regime. Once again, we can investigate the effect of diffusion on a scaling size distribution (the subscript d is for diffusion):

$$n(V) \propto V^{-B_d-1} \tag{2.18}$$

The total volume of gas available to fuel a quasi-steady state coalescence regime is therefore:

$$\int_{V_{\min}}^{V^*} n(V)\frac{\mathrm{d}V}{\mathrm{d}t}\mathrm{d}V \propto \int_{V_{\min}}^{V^*} V^{-B_d-1}V^{\epsilon}\mathrm{d}V \tag{2.19}$$

Hence, as long as $B_d < \epsilon$ the integrals are dominated by V^* and diffusive growth is dominated by the largest bubbles in the regime, supplying gas to the coalescence regime. A $B_d = \epsilon$ will supply a constant source of bubbles from the smallest sizes to V^*. As the bubble population evolves, V^* will be constantly changing, reflecting the relative efficiencies of the diffusion and coalescence dominated regimes. Since empirically, $B_d \approx 0$, even a diffusion

regime dominated by Ostwald ripening ($\epsilon = 0$) is adequate. Indeed, ultimately the result $B_d \approx 0$, may be explained as a quasi-steady-state Ostwald ripening regime.

3. Implications for number–size distributions

Fig. 4 gives a schematic diagram of various dynamic possibilities and their implications for the evolution of the number–size distribution with time, summarizing the different regimes. If the lava temperature drops before the degassing is finished, we expect $B_d \approx 0$ for the small bubbles and $B_c \approx 1$ for the medium to large bubbles. At steps 1–1′ and 2–2′, diffusion prevails. At step 3–3′, bubble growth reaches the coalescence regime; steps 4–4′–4″, 5–5′–5″, are steps of the coalescence regime associated with steady-state conditions ($\xi = 0$). When the gas source is depleted, the large bubble slope will increase, tending to an exponent $B_c = \frac{2}{3} + \gamma$ (a pure decaying coalescence regime) and with temporal scaling ($\xi = 1$). Step 6–6′ shows the development of the decaying coalescence regime. In most of the Etna

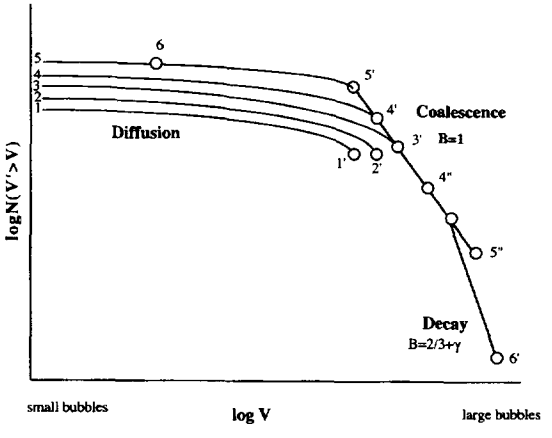

Fig. 4. Schematic diagram of log $N(V' > V)$ vs. log V. The initial diffusion-dominated regime ($B_3 \approx 0$, hence $N \approx \log V$) is indicated by the line terminating in the number 1′. A little later on, the bubbles have grown by diffusion (line terminating in 2′). Still later (3′), the largest bubbles have a coalescence time scale equal to the diffusive time scale. The steady-state coalescence regime begins between 4′ and 4″ and grows between 5′ and 5″. Finally, the diffusive gas source is depleted, and the decaying coalescence regime begins (6′).

Table 1
Gas contents from the matrix glass

Samples	F (ppm)	S (ppm)	Cl (ppm)
33a	2130± 170	40± 20	2150± 20
34a	2520± 180	50± 30	2550± 130

samples, we have observed both the diffusion ($B_d \approx 0$) and coalescence regimes ($B_c \approx 1$) associated with the quasi-steady-state conditions in most samples. We only found 2 of 24 samples with a clear lack of large bubbles and with $B > 1$. The lack of large vesicles in these samples may have several origins: (1) due to low gas content at the lava source, the decaying regime was reached quickly; (2) the large bubbles may have been lost preferentially to the atmosphere due to their higher velocity. However, this trend primarily affected only a few large vesicles, although more data are needed in the large size range. In the apparently typical case where $B_c \approx 1$ was observed for the largest bubbles, measurements of volatile concentrations in matrix glasses of the lavas suggest that gas was still diffusing as the lava cooled (Table 1). The sulphur contents for a pahoehoe sample at the source of a 1985 lava overflow and an aa sample at the front of the same overflow are low, indicating that the lavas had been previously degassed in the magma chamber and/or conduit. However, F and Cl contents both increase in the matrix glasses from the overflow source to the front (Table 1), probably as a result of microlite crystallization of anhydrous minerals (olivine, pyroxene, plagioclase and Fe–Ti oxide minerals). Microlite crystallization also may have increased the H_2O content of the lava. These data suggest that the glassy matrix was being resupplied with volatiles as the lava cooled. These volatiles could then supply gas to vesicles that were being formed.

4. Contribution of partial porosities to the total porosity

Using the model to interpret the small and large bubble regimes, we can now express the sample

vesicularity P_s as a function of the diffusion and coalescence contributions, respectively P_d and P_c:

$$P_s = P_d + P_c \tag{4.1}$$

Using our data, P_c and P_d are determined from the bubble areas. In [3] and [6], we found a simple law to transform the 2-D B exponents, found from available areas of vesicles, to 3-D B exponents valuable for volumes of vesicles. In the diffusive regime, the value $B_d \approx 0$ in 3-D space corresponds to $B_d \approx -\frac{1}{2}$ in 2-D sections, the vesicularity is expressed as (see A.4.a in [3]):

$$P_d = P(A' < A^*) = N^* A^* \frac{B_d}{B_d - 1} \tag{4.2}$$

where A^* is the largest bubble area in the diffusion regime (corresponding to V^*) and is roughly the boundary between the diffusion zone and the coalescence zone.

Table 2
Characteristic values, A^*, $A^* N^*$, largest area, A_s, in each sample, estimated total porosity, P_2, of lava samples from Mount Etna [6]; partial porosities, P_d, P_c, calculated total porosity, P_s, partial distribution numbers, N_d, N_c, of the diffusion and coalescence regimes (see text)

Sample numbers	A^* (mm^2)	A^*N^*	A_s (mm^2)	P_d(%)	P_c(%)	P_c/P_d	N_c/N_d	P_s(%)	P_2(%)	P_s/P_2
01c	0.16	0.040	15.0	1.34	18.26	13.6	0.5	19.60	13.7	1.4
07a	0.25	0.031	58.5	1.05	17.18	16.4	0.6	18.23	19.3	0.9
01b	0.40	0.032	64.0	1.06	16.13	15.2	0.5	17.19	15.7	1.1
02b	0.25	0.031	45.5	1.05	16.37	15.6	0.6	17.42	17.1	1.0
spongy	6.31		47.5							
23i	0.50	0.040	20.5	1.32	14.78	11.2	0.6	16.11	16.3	1.0
22a	0.25	0.040	22.0	1.32	17.79	13.5	0.6	19.11	19.7	1.0
22c	0.40/		7.04				0.8		5.2	
	3.16									
32a	0.25	0.040	47.0	1.32	20.76	15.7	0.6	22.09	29.9	0.7
32b	0.25	0.040	25.5	1.32	18.31	13.9	0.6	19.63	16.2	1.2
33c	0.10/		3.5				1.0		3.8	
	0.63									
33a	0.16	0.032	180.5	1.06	22.44	21.1	0.6	23.50	27.5	0.9
33b	0.40	0.040	17.5	1.33	15.18	11.4	0.8	16.51	17.2	1.0
34a	0.32	0.040	30.5	1.34	18.39	13.7	0.6	19.74	19.1	1.0
34b	0.25	0.025	56.5	0.83	13.54	16.3	0.6	14.38	17.5	0.8
46b	1.26/		28.5				0.5		24.8	1.4
	7.94									
46c	1.58	0.079	160.0	2.63	36.48	13.9	0.5	39.12	35.0	1.1
46a	2.00	0.063	100.5	2.11	24.77	11.8	0.6	26.87	33.4	0.8
45	1.58	0.100	60.5	3.32	36.32	10.9	0.6	39.64	41.5	1.0
58c	0.50	0.025	185.5	0.83	14.79	17.7	0.4	15.62	12.6	1.2
58b	0.13	0.016	30.0	0.53	8.69	16.4	0.4	9.22	6.3	1.5
58a	0.40	0.032	24.5	1.06	13.08	12.4	0.8	14.14	16.9	0.8
58d	0.79	0.063	26.5	2.09	22.04	10.5	0.6	24.13	22.8	1.1

The coalescence regime where $B_c \approx 1$ (same exponent in 2-D and 3-D spaces, see [3,6]) yields:

$$P_c = P(A' > A^*) = N^* A^* \ln \frac{A_s}{A^*} \quad (4.3)$$

where A_s is the maximum bubble size observed in the sample. With $B_d \approx -\frac{1}{2}$, Eq. (4.1) becomes:

$$P_s = N^* A^* \left(\frac{1}{3} + \ln \frac{A_s}{A^*} \right) \quad (4.4)$$

The relative contribution of P_c to P_d is:

$$\frac{P_c}{P_d} \approx 3 \ln \frac{A_s}{A^*} \quad (4.5)$$

Since empirically we find that $\frac{A_s}{A^*} \approx 10^2$–$10^3$, P_c is 13–20 times larger than P_d (Table 2). P_s is indeed close to the 2-D porosity P_2 estimated from sawn surfaces [6]. Hence, as expected, Eq. (4.4) gives a good approximation of the total porosity (i.e. there is no problem with 'outliers').

P_s is thus mainly determined by the P_c contribution and will fluctuate according to the presence or absence of large bubbles [6]. In contrast, we now show that it is, instead, diffusion which provides the largest number of vesicles to the total population. The ratio of the number of bubbles due to coalescence N_c ($= N(A > A^*)$) to the number of bubbles due to diffusion N_d ($= N(A < A^*)$) is less than unity, varying from 0.4 to 1 with an average value of 0.6 (Table 2). The model therefore predicts — in agreement with the data — two apparently contradictory characteristics: on the one hand, the total number of bubbles is dominated by the diffusion regime, whereas, on the other hand, the vesicularity is almost completely determined by the large bubble coalescence regime. The coalescence growth process is also much more rapid than other processes and may continue to larger and larger bubbles until it finally disrupts the lava, resulting in an eruption of Hawaiian or Strombolian type. Indeed, bubbles with diameters of several meters have been observed at these types of vents when the eruption rate is sufficiently high [30,31].

5. Conclusions

Previous studies on bubbles growing in near-surface lava flows involved homogeneous models (e.g., of diffusion or growth by collisions) and the characterization of the entire vesicle distributions by a single scale (e.g., by median or mean volumes). However, even at a purely empirical level, the extraordinary range of vesicle volumes — readily exceeding ratios of 10^7 — indicates that such descriptions and models can at best only very partially correspond to reality. Indeed, in a companion paper [6], which provides the direct empirical motivation for the model described here, we consider that heterogeneity occurring over wide ranges of scale is a fundamental problem and, consequently, develop appropriate statistical methods for analyzing it. Analysis of bubble sizes and vesicularity of lavas from Mount Etna over wide ranges of scale was found to show two distinct scaling regimes which form the basis of our model.

These findings lead us to propose a cascading, scaling bubble growth model based on a diffusive source, and a simple conservation law leading to the prediction that the coalescence exponent $B \approx 1$. Although this model is in fact more general, it was illustrated with the aid of the coalescence (Smoluchowski) equation. At small sizes, diffusion prevails (whether or not involving Ostwald ripening) and supplies a bubble and gas source for cascading growth by successive local collisions (coalescence) which dominates at large bubble sizes. In most cases, gas is exsolving continuously to provide a small bubble source for the large bubble indirect coalescence cascade. Exsolution can occur even with extremely small quantities of dissolved gas [19]. When the gas source is no longer effective and the dissolved gas in the matrix is depleted, a pure coalescence (decaying) regime leads to larger exponents and faster large bubble volume decay on number distribution plots. Using this model — and our analysis method — which allows us to determine the limits of the two scaling regimes, we have empirically found that coalescence contributes typically more then 90% of the total porosity, even though typically only a third of the bubbles are in the coalescence regime. These scaling distributions have

the important property of being invariant under temperature and pressure changes, leading to expansion; such expansion will simply increase or decrease all the volumes by the same factor but will not affect the exponents. This makes it possible to observe the same scaling behaviour in samples with very different pressure–temperature histories and allows scaling models to be valid under quite general conditions. Indeed, an attractive feature of the predicted power law distribution is that, unlike other statistical distributions such as exponentials, their form is conserved when samples with non-identical histories (and hence parameters) are pooled together. This, together with the fact that it naturally and simply avoids the outliers that plague other approaches, allows it also to provide very good empirical estimates of the vesicularity of each sample after identifying the characteristic V^* and N^* values of the intersection of the two power laws and the determination of the largest bubble size observed in the sample.

Our strongly non-linear model predicts the final trend of the bubble number distribution versus the volume and is expected to be very robust to changing conditions, since it requires only a few ingredients: essentially, scaling and conservation property. The bubble growth model can aid in understanding the complex physical behaviour of bubbles in basaltic lava flows. The scaling symmetries and conservation properties used in the cascade model may also apply to other quite different physical mechanisms, such as breakup of bubbles in the ocean (i.e. direct cascades), where similar exponents have been reported. Our model may also help resolve the debate on the different mechanisms suggested for bubble growth in near-surface basaltic lava flows; in particular, the degree of local versus non-local interactions between bubbles, which may be empirically and theoretically quantified by the exponant ω (Section 2.6.

Acknowledgements

This research was supported by the Natural Sciences and Engineering Research Council of Canada, the Fonds pour La Formation de Chercheurs et l'Aide à la Recherche (Québec), and the Université de Montréal. We thank B. Kerman for fruitful discussions, and S. Vergniolle for detailed comments, particularly concerning the effects of viscosity and surface tension. We also thank anonymous reviewers for critical comments. *[PT]*

Appendix A

We will demonstrate the scaling relationship that gives Eq. (2.7). Let Eq. (2.1) be written as:

$$\frac{\partial n(V,t)}{\partial t} \propto I_3(V,t) - n(V,t) I_2(V,t) \qquad (A.1)$$

where:

$$I_2(V,t) = \int_0^\infty H(V,V')\, n(V',t)\, \mathrm{d}V'$$

and:

$$I_3(V,t) = \frac{1}{2}\int_0^\infty H(V-V')\, n(V-V',t)\, n(V',t)\, \mathrm{d}V'$$

We are only interested in the scaling properties, so we will consider $I_2(\lambda V,t)$.

Even if the integral is not explicitly known, we can write:

$$I_2(\lambda V,t) = \int_0^\infty H(\lambda V,V')\, n(V',t)\, \mathrm{d}V' \qquad (A.2)$$

Introducing $V'' = \frac{V'}{\lambda}$ and using Eq. (2.2) with assumptions given in Eq. (2.3) and Eq. (2.4):

$$H(\lambda V,\lambda V'') \propto \lambda^{\gamma+\frac{2}{3}} H(V,V'') \qquad (A.3)$$

with the fact that:

$$n(\lambda V,t) \propto \lambda^{-B_c-1} n(V,t) \qquad (A.4)$$

Eq. (A.2) becomes:

$$I_2(\lambda V,t) \propto \lambda^{\gamma-B_c+\frac{2}{3}} I_2(V,t)$$

This implies:

$$I_2(V,t) \propto V^{\gamma-B_c+\frac{2}{3}} t^{-\xi} \qquad (A.5)$$

In the same way, we may find that:

$$I_3(\lambda V,t) \propto \lambda^{\gamma-2B_c-\frac{1}{3}} I_3(V,t) \qquad (A.6)$$

leading to:

$$I_3(V,t) \propto V^{\gamma-2B_c-\frac{1}{3}} t^{-2\xi} \quad (A.7)$$

The exponent of the t factor comes from the integral which involves the n^2 terms.Eq. (A.1) then becomes:

$$\frac{\partial n(V,t)}{\partial t} \propto V^{\gamma-2B_c-\frac{1}{3}} t^{-2\xi}$$

References

[1] C. Jaupart, Effects of compressibility on the flow of lava, Bull. Volcanol. 54, 1–9, 1991.

[2] C.R.J. Kilburn, Surfaces of aa flow-fields on Mount Etna, Sicily: morphology, rheology, crystallization and scaling phenomena, in Lava flows and domes, In: IAVCEI Proceedings in Volcanology, 2, J. Fink, ed., pp. 129–256, 1990.

[3] H. Gaonac'h, L'hétérogénéité de la morphologie et de la rhéologie des laves: scaling et fractales, Ph.D. Thesis, Univ. Montréal, 1994.

[4] D. Schertzer and S. Lovejoy, Nonlinear Variability in Geophysics: Scaling and Fractals, 318 pp., Kluwer, Dordrecht, 1991.

[5] H. Gaonac'h, S. Lovejoy and J. Stix, Scale invariance of basaltic lava flows and their fractal dimensions, Geophys. Res. Lett., 19, 785–788, 1992.

[6] H. Gaonac'h, J. Stix and S. Lovejoy, Scaling effects on bubble shape, size and heterogeneity of lavas from Mount Etna, J. Volcanol. Geotherm. Res., submitted.

[7] B.C. Bruno, G.J. Taylor, S.K. Rowland, P.G. Lucey and S. Self, Lava flows are fractals, Geophys. Res. Lett. 19, 305–308, 1992.

[8] B.C. Bruno, G.J. Taylor, S.K. Rowland and S.M. Baloga, Quantifying the effect of rheology on lava-flow margins using fractal geometry, Bull. Volcanol. 56, 193–206, 1994.

[9] D.K. Chester, A.M. Duncan, J.E. Guest and C.R.J. Kilburn, Mount Etna: the Anatomy of a Volcano, 404 pp., Chapman and Hall, London, 1985.

[10] D.L. Sahagian, Bubble migration and coalescence during the solidification of basaltic lava flows, J. Geol. 93, 205–211, 1985.

[11] K. McMillan, P.E. Long and R.W. Cross, Vesiculation in Columbia River basalts, Bull. Geol. Soc. Am. 239, 157–167, 1989.

[12] J.C. Aubele, L.S. Crumpler and W.E. Elston, Vesicle zonation and vertical structure of basalt flows, J. Volcanol. Geotherm. Res. 35, 349–374, 1988.

[13] D.A.M. Carbone, Analisi tessiturale quantitativa di una sezione di flusso lavico dell'eruzione etnea 1991–1993, Thesis, Univ. studi Catania, 1993.

[14] G.P. Walker, Spongy pahoehoe in Hawaii: a study of vesicle-distribution patterns in basalt and their significance, Bull. Volcanol. 51, 199–209, 1989.

[15] R.A. Wilmoth and G.P.L. Walker, P-type and S-type pahoehoe: a study of vesicle distribution patterns in Hawaiian lava flows, J. Volcanol. Geotherm. Res. 55, 129–142, 1993.

[16] A. Toramaru, Measurement of bubble size distributions in vesiculated rocks with the implications for quantitative estimation of eruption processes, J. Volcanol. Geotherm. Res. 43, 71–90, 1990.

[17] P. Sarda and D. Graham, Mid-ocean ridge popping rocks: implications for degassing at ridge crests, Earth Planet. Sci. Lett. 97, 268–289, 1990.

[18] M.T. Mangan, K.V. Cashman and S. Newman, Vesiculation of basaltic magma during eruption, Geology 21, 157–160, 1993.

[19] K.V. Cashman, M.T. Mangan and S. Newman, Surface degassing and modifications to vesicle size distributions in active basalt flows, J. Volcanol. Geotherm. Res. 61, 45–68, 1994.

[20] N.S. Bagdassarov and D.B. Dingwell, Deformation of foamed rhyolites under internal and external stresses: an experimental investigation, Bull. Volcanol. 55, 147–154, 1993.

[21] A.A. Prousevitch, D.L. Sahagian and A.T. Anderson, Dynamics of diffusive dubble growth in magmas: isothermal case, J. Geophys. Res. 98, 22283–22307, 1993.

[22] M. Manga and H.A. Stone, Interactions between bubbles in magmas amd lavas: effects of bubble deformation, J. Volcanol. Geotherm. Res. 63, 267–279, 1994.

[23] J.L. Meunier and R. Peschanski, Intermittency, fragmentation and the Smoluchowski equation, Nucl. Phys. B 324, 327–339, 1992.

[24] D.J. Tritton, Physical Fluid Dynamics, 362 pp., Cambridge University Press, Cambridge, 1985.

[25] X. Zhang and R.H. Davis, The rate of collisions due to Brownian motion or gravitational motion of small drops, J. Fluid Mechanics 230, 479–504, 1991.

[26] H. Rose and P.C. Sulem, Fully developed turbulence and statistical mechanics, J. Phys. 39, 441–484, 1978.

[27] D.J. Stein and F.J. Spera, Rheology and microstructure of magmatic emulsions: theory and experiments, J. Volcanol. Geotherm. Res. 49, 157–174, 1992.

[28] B.R. Kerman, Atmosphere–Ocean 24, 169–188, 1986.

[29] A.L. Walsh and P.J. Mulhearn, Photographic measurements of bubble populations from breaking wind waves at sea, J. Geophys. Res. 92, 14553–14565, 1987.

[30] E.A. Blackburn, L. Wilson and R.S.J. Sparks, Mechanisms and dynamics of Strombolian activity, J. Geol. Soc. London 132, 429–440, 1976.

[31] S. Vergniolle et al., Separated two-phase flow and basaltic eruptions, J. Geophys. Res. 91, 12842–12860, 1986.